Telecommunications and Radio Engineering, ?? (??):1-20 (2018)

SMART LOSSY COMPRESSION OF IMAGES BASED ON DISTORTION PREDICTION

S. Krivenko[1], O. Krylova[2], E. Bataeva[3] & V. Lukin[1]

[1]National Aerospace University (Kharkov Aviation Institute), 17, Chkalov St., Kharkiv, 61070, Ukraine

[2] Kharkiv National Medical University, Kharkiv, 61022, Ukraine

[3]Kharkov Humanitarian University "People Ukrainian Academy", Kharkiv, 61024, Ukraine

♦Address all correspondence to: V. Lukin, E-mail: lukin@ai.kharkov.com

Images of different origin are used nowadays in numerous applications spreading the tendency of world digitalization. Despite increase of memory of computers and other electronic carriers of information, amount of memory needed for saving and managing digital data (images and video in the first order) increases faster making crucial the task of their efficient compression. Efficiency means not only appropriate compression ratio but also appropriate speed of compression and quality of compressed images. In this paper, we analyze how this can be reached for coders based on discrete cosine transform (DCT). The novelty of our approach consists in fast and simple analysis of DCT coefficient statistics in a limited number of 8x8 pixel blocks with further rather accurate prediction of mean square error (MSE) of introduced distortions for a given quantization step. Then, a proper quantization step can be set with ensuring the condition that MSE of introduced errors is not greater than a preset value to provide a desired quality. In this way, multiple compressions/decompressions are avoided and the desired quality is provided quickly and with appropriate accuracy. We present examples of applying the proposed approach.

KEY WORDS: *lossy compression; image; quality; efficiency*

1. INTRODUCTION

There are numerous applications where images are employed [1-4]. To name a few, they are monitoring of the Earth and other planet surfaces [1], communications [2], visualistics and advertising [3], medical diagnostics [4], Internet of things [5]. A tendency in modern imaging and image processing systems is the increase of data amount due to many reasons as a larger size of each image, a larger amount of bits for each pixel (12- or 16-bit representations of single channel (component) images become more popular), a more often observation of objects under interest (an Earth terrain, a patient, etc.) Even if these images are not processed (e.g., filtered or classified), they

have to be saved, passed from an imager to a consumer and/or disseminated. Then, the images often have to be compressed [1, 2, 4].

As it is known, image compression techniques are divided into lossless and lossy ones [1, 2, 6-8] although sometimes near-lossy and visually lossless methods are treated as a separate subclass. A problem of lossless compression is that compression ratio (CR) is small [2, 6, 8], up to 4…5 in the most favorable cases [1] and usually considerably smaller. Moreover, for a given lossless coder, CR cannot be varied. Then, lossy image compression becomes the only alternative [1, 2, 8].

Lossy compression introduces distortions in images where more distortions relate to larger CRs. This relation is individual in the sense that the same level (for example, mean square error – MSE) of distortions can correspond to different CR [9]. This leads to different possible priorities of requirements to image lossy compression.

One typical situation is that a desired CR should be provided (e.g., one has to pass an image of a given size via a communication line during a given time interval) [2]. This was just one reason for developing the JPEG2000 standard and similar methods. There are two problems here. First, for a given CR, compressed image quality can vary in rather wide limits depending upon image complexity. For example, variations of the visual quality metric PSNR-HVS-M [10] (it is expressed in dB and its larger values correspond to better visual quality) can exceed 20 dB for the same CR and, obviously, such variations are huge [11]. The interval might include the images with PSNR-HVS-M about 40 dB when distortions are practically invisible and with PSNR-HVS-M about 20 dB when compressed images are annoying. Second, nowadays there exist image compression methods that sufficiently outperform JPEG2000 according to rate/distortion characteristics [9] and a desired CR for them can be provided quite easily due to recent advances [12, 13].

Another situation, which is more interesting in our case, is the following. Suppose that it is needed to provide a desired quality of a compressed image quite quickly in the first order and to provide a larger CR is the second order task [14-17]. Then, there are several questions that arise immediately:

1) what coder to use?

2) how to set a parameter that controls compression (PCC) to provide a desired value of a metric that characterizes quality?

3) what metric to use and what are its values for a particular application?

This paper partly answers these questions. Note that we concentrate on lossy compression techniques based on discrete cosine transform (DCT) [9, 18, 19] because they perform better than JPEG2000 in rate/distortion sense and they employ easily treatable parameters like quantization step (QS) or scaling factor (SF) as PCC.

Special attention in this paper is paid to the so called visually lossless compression [8, 19] since it is desired for many applications as compression of high quality remote sensing data [6, 8], medical images and images used in visualistics and advertisement. Certain upper level of distortions that can be introduced into such images is limited by requirement not to lose important details and diagnostic information, to preserve classification and interpretation accuracy, etc.

2. FUNDAMENTAL DEPENDENCES AND PROPERTIES IN LOSSY COMPRESSION OF NOISE-FREE IMAGES

Here we assume that one has a noise-free image $I_{ij}^t, i=1,...,I_{\text{Im}}, j=1,...,J_{\text{Im}}$ of size $I_{\text{Im}} J_{\text{Im}}$ where *ij* are pixel indices. An image after lossy compression by a given coder is denoted as $I_{ij}^c, i=1,...,I_{\text{Im}}, j=1,...,J_{\text{Im}}$. Compression is characterized by some metric calculated for the image subject to compression ($I_{ij}^t, i=1,...,I_{\text{Im}}, j=1,...,J_{\text{Im}}$) and the decompressed one $I_{ij}^c, i=1,...,I_{\text{Im}}, j=1,...,J_{\text{Im}}$.

Typical metrics used in characterization of rate/distortion performance are mean square error (MSE) and Peak Signal-to-Noise Ratio (PSNR) calculated as

$$MSE_{tc} = \sum_{i=1}^{I_{\text{Im}}} \sum_{j=1}^{J_{\text{Im}}} (I_{ij}^c - I_{ij}^t)^2 / (I_{\text{Im}} J_{\text{Im}}) , \quad (1)$$

$$PSNR_{tc} = 10 \log_{10} (255^2 / (\sum_{i=1}^{I_{\text{Im}}} \sum_{j=1}^{J_{\text{Im}}} (I_{ij}^c - I_{ij}^t)^2 / (I_{\text{Im}} J_{\text{Im}}))) , \quad (2)$$

where it is supposed that images are in 8-bit representation.

Other metrics can be used for characterizing rate/distortion performance. In particular, one can use the metric PSNR-HVS-M [10] calculated as

$$PSNR_{tc} = 10 \log_{10} (255^2 / MSE_{HVS-M}) , \quad (3)$$

where MSE_{HVS-M} is MSE calculated in 8x8 pixel blocks covering the image in DCT domain taking into account two peculiarities of human vision system (HVS), namely less sensitivity to distortions in high spatial frequencies and masking effect of texture.

Two examples of behavior of rate/distortion dependences (taken from the paper [8]) are presented in Figures 1 and 2 for conventional test grayscale images Peppers and Baboon. The former one has simple structure (a lot of quasi-homogeneous regions) whilst the latter one has complex structure (is almost fully textural). The dependences are presented for CR from 8 till 64 (sometimes, till 32), i.e. in typical range for CR values. Three compression methods are considered: JPEG with uniform quantization; SPIHT that can be treated as analog of JPEG2000; and modification of ADCT coder called ADCT-M intended to provide high visual quality due to non-uniform quantization of DCT coefficients [9].

In accordance with the theory, all dependences are monotonously decreasing. But there are sufficient differences in them that can be, in general, summarized as follows:

1) PSNR values are slightly better for SPIHT for CR about 10; later, for larger CR, the best PSNR values are provided by ADCT-M; JPEG is the worst;

2) The best PSNR-HVS-M values are provided by ADCT-M, the benefit compared to other coders is considerable, a few dB; this shows that a sufficient benefit in visual quality of compressed images can be provided by modern compression techniques like ADCT-M (see also data in [9]).

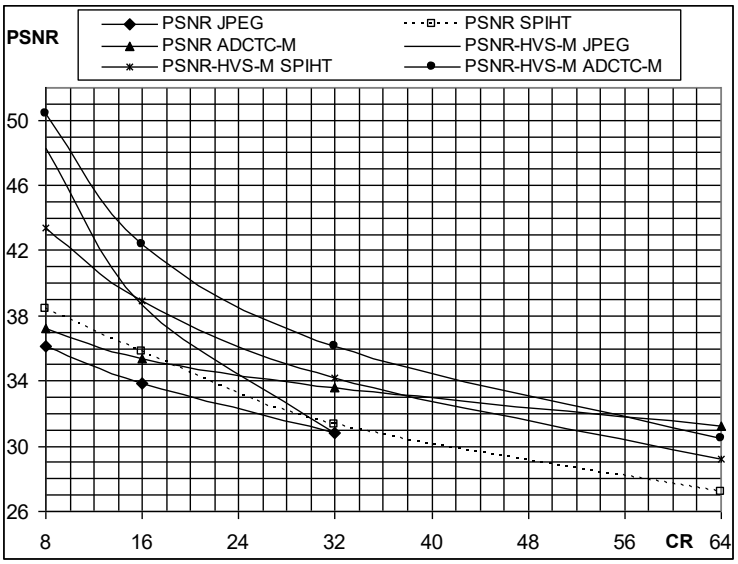

Fig. 1. Dependences of PSNR and PSNR-HVS-M vs CR for three coders for the test image Peppers

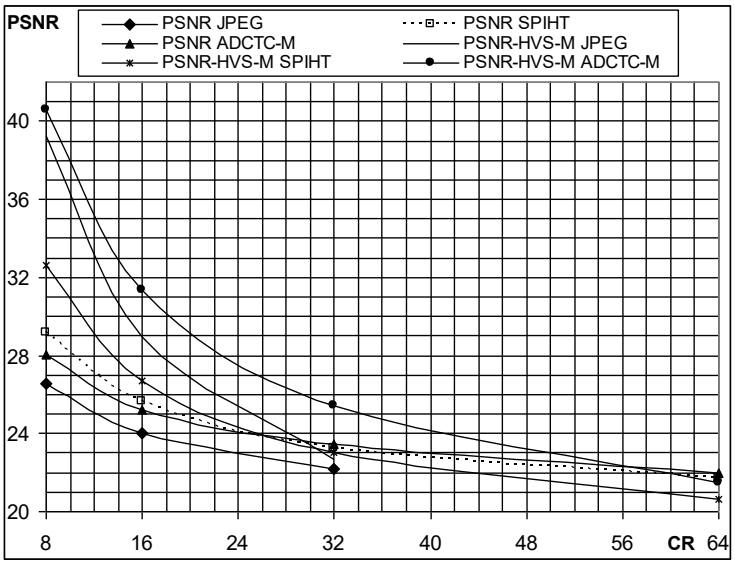

Fig. 2. Dependences of PSNR and PSNR-HVS-M vs CR for three coders for the test image Baboon

An important observation is that for CR=8 the PSNR values are about 37 dB for the test image Peppers and about 28 dB for the test image Baboon showing that MSEs of degradations differ a lot. The degradations are obviously larger for the image with a more complex structure. This happens for all three considered coders. Moreover, this takes place for all coders and this is the problem not only in image compression but also in video compression with the fixed bitrate [9].

To solve this problem, iterative compression/decompression with control of image quality after each iteration step and further PCC adjusting can be applied.

Advantages of this procedure are the following [9]:

1) It is applicable for any quality metric under condition that dependence of this metric on PCC is monotonous (this condition is usually valid although it should be checked in advance for any studied coder and any considered metric);

2) Usually high accuracy of providing a desired value of a used metric can be reached; for example, it is usually possible to provide a desired PSNR or PSNR-HVS-M with error less than 0.2 dB and this is appropriate for practice.

Meanwhile, iterative procedure has several drawbacks, namely:

1) It is a priori unknown how many iteration steps will be needed to carry out compression of a given image with a desired quality according to a chosen metric by a given coder; it is shown in [9] that 10 iteration steps (and sometimes even more) are possible;

2) Parameters of iteration procedure (initial value of PCC and its step, accuracy of metric providing) should be reasonably chosen; however, such settings can, on the average, decrease the number of iteration steps;

3) Large time for completing iterations is needed if a used compression/decompression technique is not fast enough; for example, the coder ADCT-M performs partition scheme optimization and image compression is blocks of content-adaptive size; then, on one hand, better quality of compressed images is provided (see the data above), but, on the other hand, considerably more time is needed for both compression and decompression.

Some propositions concerning how to diminish the number of iteration steps can be found in the paper [9]. In particular, the starting PCC value can be set based on a priori collected statistics. Below we present one example borrowed from [9]. Fig. 3 represents averaged dependences of QS on the quality metric (PSNR-HVS-M in the considered case) for two DCT-based coders, AGU [18] and ADCT [19] (recall that AGU performs in 32x32 pixel blocks and carries out deblocking after decompression). As it is seen, QS about 17 for the coder AGU provides compression with, on the average, PSNR-HVS-M about 41 dB, i.e. with practically invisible distortions. However, values of PSNR-HVS-M for particular images vary in rather wide limits, from 39 dB to 46 dB (see data in [9], Fig. 14). Meanwhile, it is usually desired to provide PSNR-HVS-M with error less than 0.5 dB. Thus, even if the starting QS is set properly, iterations are needed.

Fig. 4 presents averaged dependences of QS on PSNR-HVS-M for two DCT-based coders, AGU-M and ADCT-M which are modifications of AGU and ADCT, respectively, that take into account peculiarities of HVS [9] by quantizing higher

spatial frequencies with larger quantization steps (these steps are determined by a set SF and special matrixes). For these coders, the problem is the same. For example, to provide the desired PSNR-HVS-M=41 dB, one has to employ SF about 10 (see data in Fig. 4). But, in fact, setting the fixed SF=10 for the coder AGU-M provides PSNR-HVS-M in the limits from 40 to 44 dB. Thus, additional adjusting SF is needed.

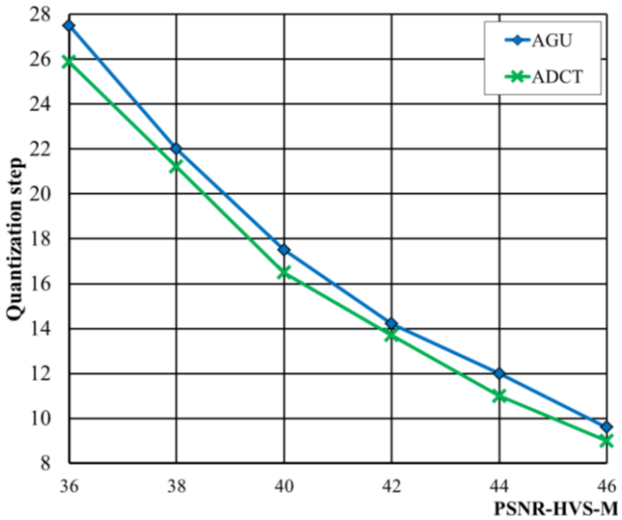

Fig.3. Averaged (for many 8-bit test images) dependence of QS on PSNR-HVS-M for the coders AGU and ADCT

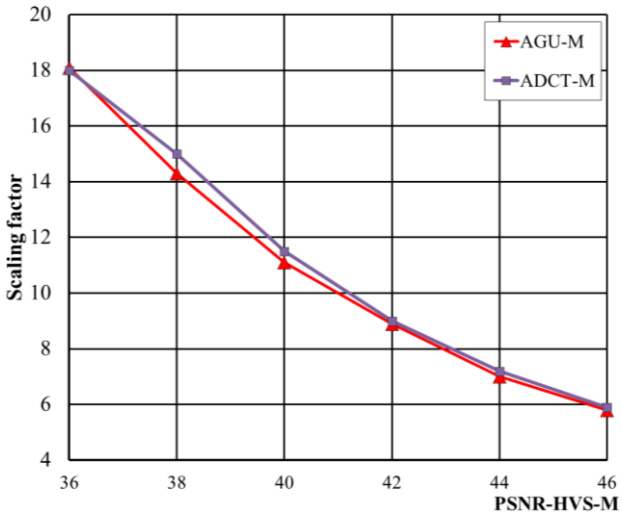

Fig.4. Averaged (for many 8-bit test images) dependence of SF on PSNR-HVS-M for the coders AGU-M and ADCT-M

Iterative procedures with the recommended step of QS changing $\Delta QS=2$ [9] need a few steps to provide a desired PSNR-HVS-M in both considered examples.

However, this does not fully solve the problem and it is still desirable to have a one-step (or, in the worst case, a two-step) procedure for compressing an image with a desired quality.

3. ANALYSIS OF REASONS OF DISTORTION PARAMETER VARIATION

Similarly to the well-known JPEG, it is clear that distortions in DCT-based lossy compression of images are due to quantization of DCT coefficients [2, 20]. If the total number of 8x8 pixel blocks is N, then suppose that one has DCT coefficients $D(n,k,l), n=1,...,N; k=0,...,7; l=0,...,7$. After quantization one has the coefficients $D_q(n,k,l), n=1,...,N; k=0,...,7; l=0,...,7$ and

$$MSE = \frac{1}{N}\sum_{n=1}^{N} MSE_n = \frac{1}{64N}\sum_{n=1}^{N}\sum_{k=0}^{7}\sum_{l=0}^{7}(\Delta D_q(n,k,l))^2 \quad (4)$$

where

$$D_q(n,k,l) = [D(n,k,l)/QS], k=0,...,7; l=0,...,7,$$

$$\Delta D_q(n,k,l) = QS \times D_q(n,k,l) - D(n,k,l), k=0,...,7; l=0,...,7.$$

Here $[\bullet]$ denotes rounding-off to the nearest integer, n is the block index.

It is usually assumed that quantization errors have uniform distribution and, due to this, their variance is $\Delta^2/12$ where Δ is interval size. Since in our case Δ=QS, it is possible to expect that MSE of introduced variance (for uniform quantization of DCT coefficients) should be about $QS^2/12$. However, a more detailed analysis shows that this is not true (at least, it is not true quite often).

First, let us analyze dependence of MSE of introduced losses on QS for three test images: noise-free test remote sensing images Frisco (that has simple structure) and Airfield (that has a more complex structure) and the test image Frisco corrupted by additive white Gaussian noise. The dependences are presented in Fig. 5 for the coder ADCT.

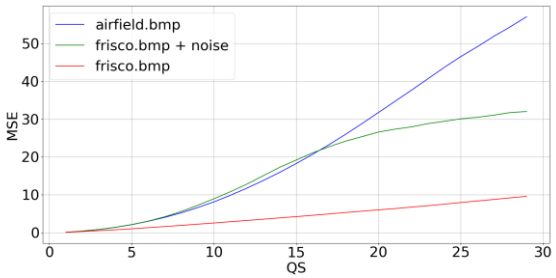

Fig. 5. Dependences $MSE_{out}(QS)$ for noise-free and noisy images Frisco and noise-free image Airfield

The first observation is that there is a sufficient difference in MSE (especially for QS>5) depending upon image complexity. The second observation is that noise presence changes behaviour of MSE compared to the same noise-free image.

Fig. 6 shows dependences of $CR(QS)$ for the same three images. It is seen that the noise-free image with the simple structure is compressed much better than two others for the same QS. The main reason is that for noise-free simple structure image there are considerably more zero values of DCT coefficients after their quantization.

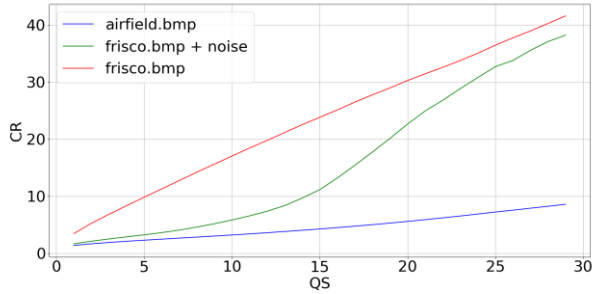

Fig. 6. Dependences $CR(QS)$ for noise-free and noisy images Frisco and noise-free image Airfield

The reason for these effects is in distributions of AC DCT coefficients. They are presented in Fig. 7 in the same scale for all three images. Distributions for noise-free images are not Gaussian and the distribution for the simpler structure image is considerably narrower. Noise presence (especially if its variance is rather large) makes the distribution closer to Gaussian and wider.

Such differences in distributions of AC DCT coefficients result in differences of distributions of quantization errors. If QS is small compared to the distribution "width" (scale), one has distribution of quantization errors close to uniform (the examples are given in Figures 8,a and 8,d). This happens for rather small Q, complex structure and/or noisy images. Then, MSE of introduced errors should be close to $QS^2/12$.

Meanwhile, if the distribution of AC DCT coefficients is narrow compared to QS, the distribution of quantization errors can sufficiently differ from uniform. Examples are given in Figures 8,b and 8,c. This happens for simple structure images that are not corrupted by the noise. Then, MSE of introduced errors is expected to be smaller than $QS^2/12$. Thus, we can guess that MSE of introduced distortions somehow depends upon statistics of DCT coefficients that, in turn, is determined by image and noise properties.

Statistics of AC DCT coefficients analyzed above has been collected in 8x8 pixel blocks but dependences are analyzed for compression techniques that employ blocks of other size. Possibility of such analysis has been proven in [20] where it has been shown that MSE predicted for a given QS for a set of 8x8 pixel blocks is in high correlation with MSE for AGU and ADCT coders. Moreover, the set of blocks in which statistics is collected can be of limited size. In other words, there is no need to collect statistics of AC DCT coefficients for all possible positions of blocks. These

observations (see [20] for more details) have opened perspectives for providing a desired MSE or PSNR faster [16, 17, 21].

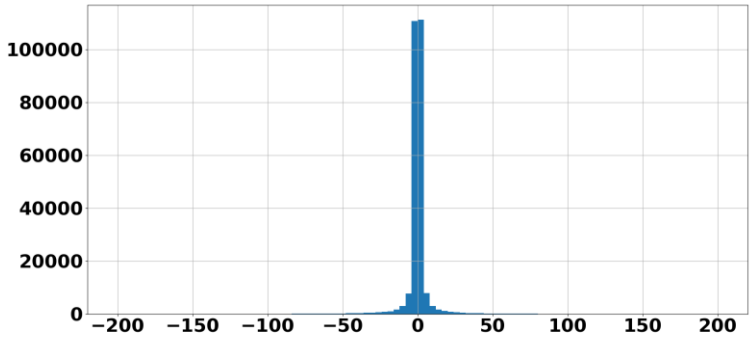

a

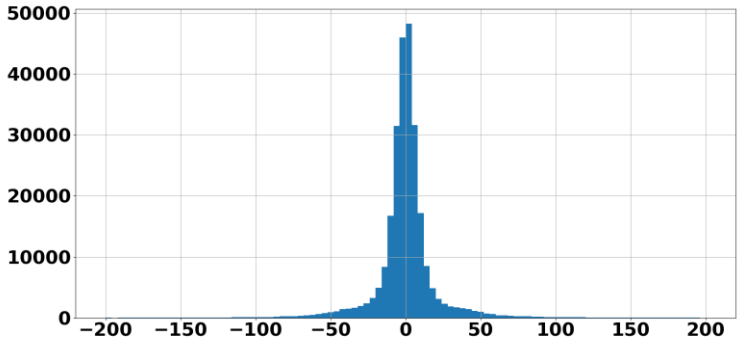

b

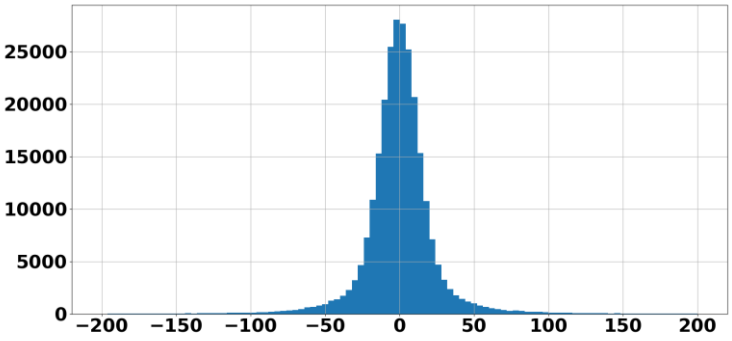

c

Fig. 7. Distributions of AC DCT coefficients for the noise-free image Frisco (a), noise-free image Airfield (b) and noisy image Airfield (c), the limits are from -200 to 200

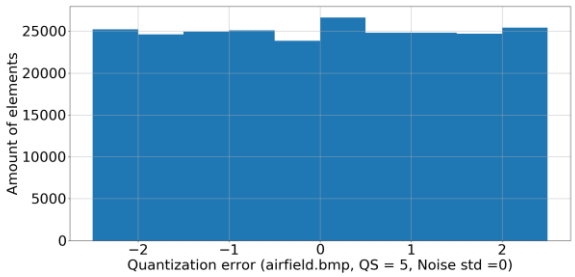

a

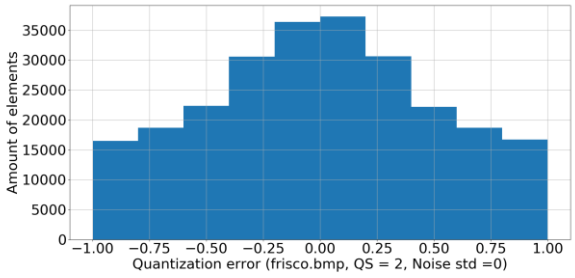

b

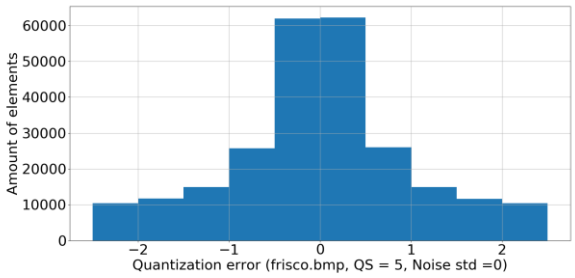

c

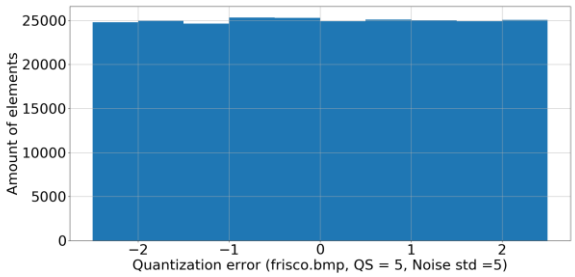

d

Fig. 8. Examples of histograms of quantization error for AC DCT coefficients (see comments under each histogram)

4. COMPRESSION PARAMETER PREDICTION

Let us first explain what is our idea and what is meant by compression parameter prediction. Suppose the following. Having an image to be compressed and carrying out some simple and fast analysis of its statistics, it is possible to calculate an approximate (predicted) value of a considered metric characterizing compression for a given coder and a PCC used in this coder. As example – suppose that analyzing statistics of DCT coefficients in a set of blocks it is possible to calculate approximate MSE for a given QS for AGU or ADCT coders. Then, it becomes possible to adjust PCC (QS in our case) in such a manner that a predicted value of the considered metric (e.g., MSE) is approximately equal to a desired value of this metric (e.g., MSE_{des}=25 for 8-bit images that approximately corresponds to the threshold of invisibility of introduced distortions [11]. If these assumptions are valid and the corresponding algorithm can be realized, it becomes possible to carry out compression with a desired quality without compression/decompression iterations.

Before starting to study possible approaches to prediction, it is worth recalling the relating pre-history. An attempt to predict PSNR for JPEG was done in [14]. The authors assumed the following: distribution of AC DCT coefficients is close to Laplacian. Then, estimating this distribution scale S and having a priori obtained dependence of quantization error MSE on the ratio QS/S or SF/S, it is possible to predict MSE (or PSNR). It was proposed to carry out scale estimation having AC DCT coefficients calculated in all blocks of an image subject to compression.

This approach has several shortcomings. First, it has been developed only for JPEG. Second, it was supposed that all AC DCT coefficients have to be collected and saved to estimate distribution scale (this is not a serious problem since, in fact, scale estimation can be done without saving all DCT coefficients). Third, the assumption that distribution of AC DCT coefficients is close to Laplacian is not valid. Due to this, MSE and PSNR for a given QS are predicted with errors. For PSNR, the errors do not exceed 1 dB and this can be acceptable for practice. Since all DCT coefficients in 8x8 pixel blocks have to be calculated for prediction, prediction takes almost the same time as compression and, in fact, prediction is the embedded part of JPEG compression.

This cannot be the case for compression techniques AGU and ADCT. For them, it is desired to carry out prediction faster. Two ways to do so have been proposed in our papers [15, 20]. The first idea is that predicted MSE for advanced DCT-based coders (AGU, AGU-M, ADCT, ADCT-M) can be calculated as predicted MSE for JPEG multiplied by the corresponding correcting factor (the values of these factors are close to unity). The second idea is that prediction can be done as (for uniform quantization)

$$MSE_{pred} = \frac{1}{R}\sum_{r=1}^{R} MSE_r = \frac{1}{64R}\sum_{r=1}^{R}\sum_{k=0}^{7}\sum_{l=0}^{7}(\Delta D_q(r,k,l))^2, \quad (5)$$

$$\Delta D_q(n,k,l) = QS \times D_q(r,k,l) - D(r,k,l), k = 0,...,7; l = 0,...,7, r = 1,...,R \quad (6)$$

where R denotes the number of considered blocks which is sufficiently smaller than the total number of 8x8 pixel blocks $N = I_{\mathrm{Im}} J_{\mathrm{Im}} / 64$ covering a compressed image in

non-overlapping manner. It is shown in [15, 20] that R can be by ten times smaller than N and it is often enough to have 300…500 randomly chosen blocks to assess statistics of AC DCT coefficients with appropriate accuracy.

Note that (5) and (6) allow predicting MSE for a given QS but does not give direct answer how to provide MSE_{des}. One way out can be to use an iterative procedure of QS setting to produce predicted MSE close to MSE_{des} with appropriate accuracy. This can be iterative procedures similar to [9] applied to adjust QS using (5) but without image compression/decompression, i.e. considerably faster. An error equal to 5% of MSE_{des} can be considered as appropriate accuracy (stopping rule).

Summarizing this description, we have to state that simplicity and a rather high speed of setting QS to provide MSE_{des} is ensured by the following. First, 2D DCT has to be performed in 8x8 pixel blocks for which there exist numerous efficient hardware and software realizations [22]. Second, a limited number of blocks which is smaller than the total number of 8x8 pixel blocks for a given image is analyzed. Third, even if 8…10 iterations are needed to find the desired QS, operations in (5) and (6) are quite simple, fast and they can be easily realized.

Meanwhile, this stage can be additionally accelerated. This can be done using a prediction approach that has been originally put forward in [16] and then further developed in [17, 21]. The idea is the following. Suppose that a given metric can be approximated as and rather simple function of PCC (e.g., QS) and one or two parameters that describe distribution of AC DCT coefficients where these parameter(s) can be calculated very easily and quickly. A general particular formula for MSE_{pred} is

$$MSE_{pred} = (QS^2 / 12) f_0(X) \tag{7}$$

where $f_0(X)$ is a function of parameters X (or one parameter).

Then, our task is to find this function and to decide what parameter(s) to use as its argument(s). The task has been solved using scatter-plots and regression as well as previous experience [23]. Suppose that we have a set of test images that are compressed by a considered coder with different QS values. For each compression case, MSE of introduced distortions is measured, the parameter(s) X are determined and QS is known. Then, each case can be represented as the scatter-plot point where vertical axis corresponds to $\hat{f}_0(X) = 12MSE / QS^2$ and horizontal axis (or axes) relate to X. An example of such scatter-plot where X is one parameter is shown in Fig. 9 (the coder is ADCT). As parameter characterizing AC DCT coefficient statistics we have used P_0 – probability that DCT coefficients after quantization become equal to zero. This parameter can be also treated as probability that absolute values of $D(r,k,l)), r = 1,...,R; k = 0,...,7; l = 0,...,7$ are smaller than QS/2. It is clear that P_0 can be very easily and quickly calculated and this makes prediction faster than prediction based on (5) and (6).

The parameter P_0 has been chosen based on previous experience [12, 13] where this parameter has been employed to predict CR (see the scatter-plot in Fig. 10). The

points are placed in a very compact manner and this shows that there is a very strict dependence between CR and P_0 that allows accurate prediction of CR.

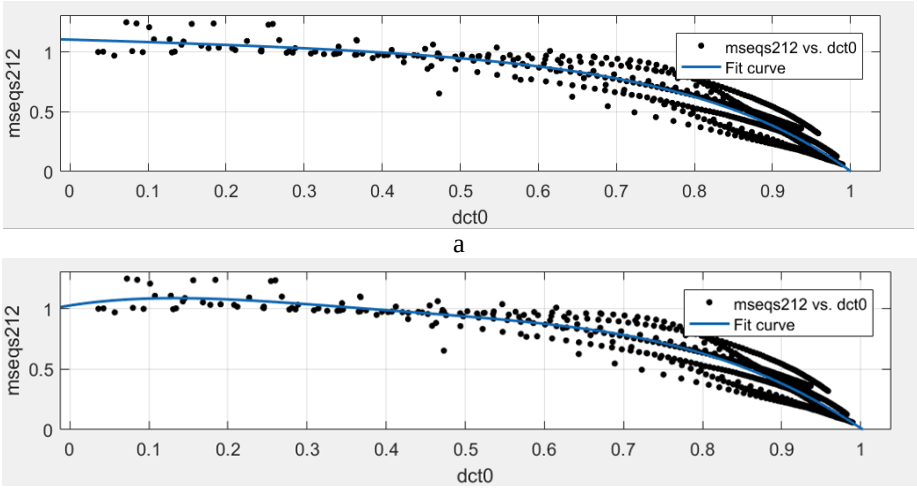

Fig. 9 Scatter-plot of $MSE/(QS^2/12)$ vs P_0 for noise-free images and two variants of fitted curves, ADCT coder

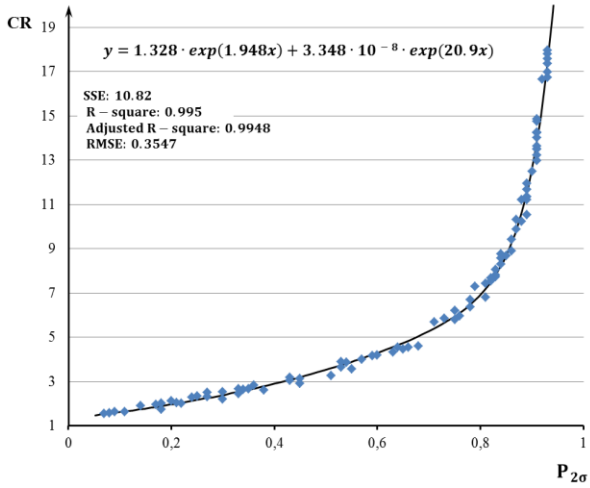

Fig. 10. The scatter-plot of CR on P_0 and the fitted curve

Let us verbally explain how P_0 describes the image properties. For a given QS, P_0 is smaller if the scale of AC DCT coefficients is larger, i.e. if image complexity is higher (and then CR is smaller as it follows from Fig. 10, this is in good agreement with the plots in Fig. 6). Thus, this shows that P_0 is the parameter that characterizes image complexity in a rather good and adequate manner.

Now let us come back to the scatter-plots in Fig. 9 (the scatter-plots in Figures 9,a and 9,b are the same but the fitted curves are different). The scatter-plot is rather

"compact" and this indicates that we can approximate the function well enough. It is possible to divide the interval of possible arguments (from 0 to 1) into two regions (subintervals). The first subinterval is P_0<0.6 where better compactness of scatter-plot points is observed and the estimates $\hat{f}_0(P_0)$ are close to unity. This means that for P_0<0.6 we have $MSE_{pred} \approx QS^2/12$ and, thus, $QS_{des} = \sqrt{12MSE_{des}}$. Then, to provide invisibility of distortions that usually takes place for MSE about 20…25 one has to use QS about 17 for the coders AGU and ADCT. This occurs to be in perfect agreement with data in Fig. 3. Keeping in mind that to provide the same quality the coders AGU-M and ADCT-M have to use $SF_{des} \approx QS_{des}/1.6$ compared to AGU and ADCT, we have the recommendation of providing invisibility of distortions for AGU-M and ADCT-M – they have to use $SF_{des} \approx 10.5$. This is in quite good agreement with empirical recommendations given in [8]. It was proposed there to set $SF \approx (I_{\max} - I_{\min})/20$ for AGU-M where $I_{\max}, I_{\min}$ are maximal and minimal values of an image to be compressed. For 8-bit images, $I_{\max} - I_{\min}$ is usually slightly smaller than 255 and, thus, we get $SF_{des} \approx 12$. MSE in the early paper [8] is calculated as $(I_{\max} - I_{\min})^2/2000 \approx 30$, i.e. slightly larger than MSE that we recommend now (20…25). Note that if P_0<0.6 , then CR<6 (see data in Fig. 10).

There is also the subinterval $P_0 \geq 0.6$ (Fig. 9) that corresponds to larger CR (see Fig. 10) and larger introduced distortions. The scatter-plot points are placed more sparsely than for P_0<0.6. However, in any case the tendencies and properties are seen well. First, MSE of introduced distortions are smaller or sufficiently smaller than $QS^2/12$. In other words, MSE increases slower that proportionally to QS^2 with QS increasing. Particular examples of this can be seen in Fig. 5. Since for a given QS the probability P_0 is larger for simpler structure images, this means that such images can be compressed with a larger CR than complex structure images for the same MSE of introduced distortions. This conclusion is in agreement with observations presented above in Section 2.

Here we have to briefly discuss the curve fitting into scatter-plots as well as peculiarities of scatter-plot formation. There is a well-developed theory of regression and criteria of fitting quality [24]. The most known of then are goodness-of-the-fit (usually denoted as R^2) and root mean square error (RMSE). R^2 for compact data and good fitting tends to unity whilst RMSE has to be as small as possible.

An important point is also the scatter-plot forming. While getting data for a scatter-plot, one has to take into account some recommendations. First, arguments of points should cover the entire interval of their possible values. Second, data should represent a variety of situations possible in practice. In our case, this means that the test image set has to include simple, moderate and complex structure images and QS has to be varied in very wide limits. These recommendations have been taken into account in getting the scatter-plots in Figures 9 and 10.

Another question is choosing functions for fitting. Nowadays Matlab and Excel contain blocks that allow solving the tasks of finding a proper function and

determining its parameters easily. For our task, we have to find a rather simple function and several choices have been analyzed. In particular, we checked polynomials of different order, sums of exponentials, power functions, short Fourier series. Since in our case (see Fig. 9) the function has to be about unity for P_0<0.6 and then to monotonously decrease for larger P_0, its choice is not a problem. Several functions can be good solutions. In particular, the sum of two exponentials (Fig. 9,a) and short Fourier series (Fig. 9,b) produce similar results. In both cases, R^2 is about 0.92 (this is considered to be a good result in regression) and RMSE is 0.084 (that shows rather high accuracy of prediction). We recommend applying

$$f_0(P_0)=-0.007721\exp(4.824P_0)+1.112\exp(-0.1455P_0). \quad (8)$$

Having this approximation, we propose the following procedure to provide $\mathrm{MSE}_{\mathrm{des}}$:

1) Start from some QS_o; as $QS_{des}=\sqrt{12MSE_{des}}$ we recommend using $QS_0=\sqrt{12MSE_{des}}$; calculate P_0 for this QS_0 by comparing absolute values of the considered AC DCT coefficients to $Q_0/2$.

2) If P_0<0.6, use QS_0 as QS_{des} and stop the procedure.

3) Otherwise, increase (change) QS and calculate P_0 for it until $QS^2 f_0(P_0)\in[11MSE_{des};13MSE_{des}]$ (the interval width is chosen to provide fast convergence and appropriate accuracy). Then, use this QS as QS_{des} and stop the procedure. QS can be increased by about $0.08\,QS_0$ at each next step.

The proposed procedure usually needs not more than 3 steps to find QS_{des}. The main computation time at each step is taken by the operation of calculating P_0 which is very simple and fast. Certainly, no compression/decompression is needed.

Above we have paid main attention to predicting MSE for coders where QS is used as PCC. These are coders AGU and ADCT for which the scatter-plots and main dependences are very similar [16, 21]. It might seem that the presented results are of importance only for the metric MSE, the aforementioned coders, and grayscale images. However, this is not so.

First of all, it has been shown in [20] that prediction of MSE can be done based on (5) for the coders AGU-M and ADCT-M. The only difference in this case is that non-uniform quantization is used and a given SF determines individual quantization steps $QS(k,l),k=0,...,7;l=0,...,7$ for each spatial frequency. Then, in each *r*-th block

$$D_q(r,k,l)=[D(r,k,l)/QS(k,l)],k=0,...,7;l=0,...,7, \quad (9)$$

$$\Delta D_q(r,k,l)=QS(k,l)\times D_q(n,k,l)-D(r,k,l),k=0,...,7;l=0,...,7,r=1,...,R. \quad (10)$$

and (10) should be used instead of (6) for calculating MSE according to (5). Obviously, the difference is not essential for speed of calculations. Correcting factors

given in [20] and approximately equal to 0.9 for both coders should be taken into account in MSE predicting for AGU-M and ADCT-M. In addition, we believe that MSE prediction using scatter-plots and curve fitting can be done for the coders AGU-M and ADCT-M similarly to AGU and ADCT.

Second, since MSE can be predicted, PSNR can be predicted as well. This can be done indirectly, by prediction of MSE. However, prediction can be also done directly. The predicted PSNR can be presented as

$$PSNR_{pred} = 10\log_{10}(255^2 / ((QS^2/12) f_0(P_0)) = \\ = 58.92 - 20\log_{10}(QS) + f_1(P_0), dB \quad (11)$$

where $f_1(P_0) = -10\log_{10}(f_0(P_0))$. The scatter-plot is given in Fig. 11. According to (11) and if $P_0 < 0.6$, there is almost linear decreasing of $PSNR_{pred}$ with $\log_{10}(QS)$.

We believe that prediction is also possible for other metrics. At least, we plan to predict the metric PSNR-HVS-M.

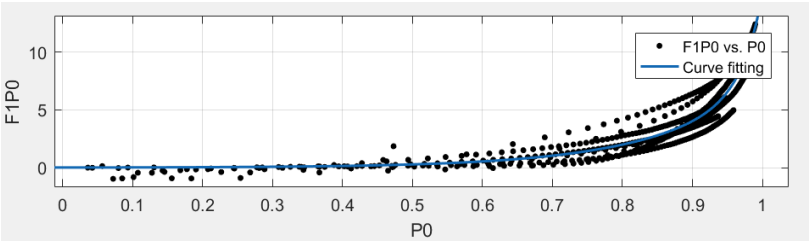

Fig. 11. Scatter-plot of $f_1(P_0)$ for noise-free images and the fitted curve, ADCT coder

Third, the scatter-plots above have been obtained for grayscale test images that are typical optical or remote sensing images. However, very similar scatter-plots have been obtained for medical (retina) images (see Fig. 12 and compare the scatter-plot to scatter-plots in Fig. 9).

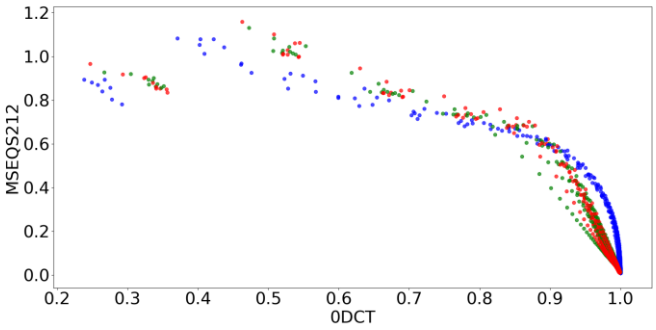

Fig. 12. Scatter-plot of $f_0(P_0)$ for component images of color retina images and the fitted curve, AGU coder

Fig. 13 presents the result of compressing retina color image without visible distortions, i.e. all diagnostically valuable information is preserved. Since this image does not have a lot of textures and detail and due to the use of 3D version of AGU coder that employ inter-channel correlation, the attained CR slightly exceeds 100. This shows how large can be gain in medical data volume due to their smart lossy compression. So, the approach is applicable to different types of images and is quite universal.

a

b

Fig. 13. Original (a) and compressed (b) retina images

Finally, let us analyse an example for natural scene image (the test image Goldhill). In Fig. 14 we represent the original noise-free image and its compressed

versions with MSE=20, 40, and 60. As it is seen, the difference between images in Figures 14,a and 14,b can be hardly found whilst distortions are noticeable in Fig. 14,c and well seen in Fig. 14.d. This demonstrates expedience of using the designed approach for different applications.

a b

c d

Fig. 14. Compression results for the test image Goldhill: noise-free uncompressed image (a), image compressed with MSE=20 (CR=11.5, PSNR-HVS-M=38.1 dB) (b); image compressed with MSE=40 (CR=23.9, PSNR-HVS-M=32.6 dB) (c); image compressed with MSE=60 (CR=40.1, PSNR-HVS-M=29.5 dB) (d)

5. CONCLUSIONS

The problem of fast lossy compression of images of different origin with providing a desired quality (often, invisibility of introduced distortions) is considered. It is shown that there are quite clear dependences of quality metrics on QS and SF for DCT-based lossy coders. These metrics considerably depend on image properties. This allows predicting metric values quickly and quite accurately by computing and processing image statistics in DCT domain. Then, it becomes possible to quickly determine QS or SF for providing a desired quality. The proposed approach is general and can be applied for different types of images in medical practice, visualistics, remote sensing, robotics, etc.

REFERENCES

1. Blanes, I., Magli, E., Serra-Sagrista, J., (2014) A Tutorial on Image Compression for Optical Space Imaging Systems, *IEEE Geoscience and Remote Sensing Magazine*, 2(3), pp. 8-26.
2. Taubman, D., Marcellin, M., (2002) *JPEG2000 Image Compression Fundamentals, Standards and Practice*, Springer, Boston: Kluwer, 777 p.
3. Bataeva, K.V., (2015) Analysis of advertisement gender images in social-iconographic context, *Actual Problems of Philosophy and Sociology*, 5, pp. 15-21.
4. Prince, Jerry L., Links, Jonathan., (2005) Medical Imaging Signals and Systems, *Pearson Cloth*, 496 p.
5. Vongsingthong, S., Smanchat, S., (2014). Internet of Things: A review of applications & technologies. *Suranaree Journal of Science and Technology*, 37 p.
6. Aiazzi, B., Alparone, L., Baronti, S., Lastri, C., Selva, M., (2012) Spectral Distortion in Lossy Compression of Hyperspectral Data, *Journal of Electrical and Computer Engineering*, 2012, Article ID 850637, 8 p.
7. Lee, C., Youn, S., Baek, J.Y., Sagristà, J.S., (2015) Effects of compression on classification performance and discriminant information preservation in remotely sensed data, *Proc. of Satellite Data Compression, Communications, and Processing XI*, 950103, doi: 10.1117/12.2180223.
8. V. Lukin, M. Zriakhov, S. Krivenko, N. Ponomarenko, Z. Miao, Lossy compression of images without visible distortions and its applications, Proceedings of ICSP 2010, Beijing, October, 2010, pp. 694-697.
9. Zemliachenko, A., Ponomarenko, N., Lukin, V., Egiazarian, K., Astola, J., (2015) Still Image/Video Frame Lossy Compression Providing a Desired Visual Quality, *Multidimensional Systems and Signal Processing*, 22 p. DOI:10.1007/s11045-015-0333-8.
10. Ponomarenko, N., Silvestri, F., Egiazarian, K., Carli, M., Astola, J., Lukin, V., (2007) On between-coefficient contrast masking of DCT basis functions, *CD-ROM Proc. of VPQM*, USA, 4 p.
11. Lukin, V., Ponomarenko, N., Egiazarian, K., Astola, J., (2015) Analysis of HVS-Metrics' Properties Using Color Image Database TID2013, Proc. of ACIVS, Italy, pp. 613-624.
12. Zemliachenko, A., Abramov, S., Lukin, V., Vozel, B., Chehdi, K., (2016) Improved Compression Ratio Prediction in DCT-based Lossy Compression of Remote Sensing Images, *Proc. of IGARSS*, Beijing, China, 4 p.
13. Zemliachenko, A., Kozhemiakin, R., Vozel, B., Lukin, V., (2016) Prediction of Compression Ratio in Lossy Compression of Noisy Images, Proc. of TCSET 2016, Lviv-Slavske, Ukraine, pp. 693-697.
14. Minguillon, J., Pujol, J., (2001) JPEG Standard Uniform Quantization Error Modeling with Applications to Sequential and Progressive Operation Modes, *Electron. Imaging*, 10(2), pp. 475-485.
15. Kozhemiakin, R., Lukin, V., Vozel, B., (2017) Image Quality Prediction for DCT-based Compression, *Proc. of CADSM 2017*, Ukraine, pp. 265-268.

16. Krivenko, S., Lukin, V., Zriakhov, M., Vozel, B., (2018) MSE Prediction in DCT-based lossy compression of Noise-free and Noisy Remote Sensing, *Proceedings of TCSET*, Lviv-Slavsko, Ukraine, pp. 883-888.
17. Krivenko, S., Lukin, V., Krylova, O., Shutko, V. (2018) Visually Lossless Compression of Retina Images, *Proceedings of Elnano*, in press.
18. Ponomarenko, N., Lukin, V., Egiazarian, K., Astola, J., (2005) DCT Based High Quality Image Compression, *Proc. of 14th Scandinavian Conference on Image Analysis*, 14, pp. 1177-1185.
19. Ponomarenko, N., Lukin, V., Egiazarian, K., Astola, J., (2008) ADCT: A new high quality DCT based coder for lossy image compression, *CD ROM Proc. of LNLA*, Switzerland, 6 p.
20. Vozel, B., Kozhemiakin, R., Abramov, S., Lukin, V., Chehdi, K., (2017) Output MSE and PSNR prediction in DCT-based lossy compression of remote sensing images, *Proc. SPIE. 10427, Image and Signal Processing for Remote Sensing XXIII*, Warsaw, Poland, September 2017, 11 p.
21. Krivenko, S., Zriakhov, M., Lukin, V., Vozel, B., (2018) MSE and PSNR Prediction for ADCT Coder Applied to Lossy Image Compression, *IEEE 9th International Conference on Dependable Systems, Services and Technologies (DESSERT)*, Kiev, Ukraine, pp. 613 – 618.
22. Kitsos, P., Voros, N. S., Dagiuklas, T., Skodras, A. N., (2013) A high speed FPGA implementation of the 2D DCT for ultra high definition video coding, Proc. 18th Int. Conf. Digit. Signal Process. (DSP), pp. 1-5.
23. Abramov, S., Krivenko, S., Roenko, A., Lukin, V., Djurović, I., Chobanu, M., (2013) Prediction of filtering efficiency for DCT-based image denoising, *Proc. of MECO 2013*, Budva, Montenegro, pp. 97-100. DOI: 10.1109/MECO.2013.6601327MECO 2013.
24. Cameron, C. , Windmeijer, A., Frank, A.G., Gramajo, H., Cane, D.E., Khosla, C., (1997) An R-squared measure of goodness of fit for some common nonlinear regression models, *J. of Econometrics*, 77(2), 16 p.